Astron. Astrophys. 361, 480–490 (2000)

ASTRONOMY AND ASTROPHYSICS

Flat radio-spectrum galaxies and BL Lacs

I. Core properties

J. Dennett-Thorpe[1,2] **and M.J. Marchã**[2]

[1] Kapteyn Institute, Postbus 800, 9700 AV Groningen, The Netherlands
[2] Observatório Astronómico de Lisboa, Tapada da Ajuda, 1300 Lisbon, Portugal

Received 14 March 2000 / Accepted 14 July 2000

Abstract. This paper concerns the relationship of BL Lacs and flat–spectrum weak emission–line galaxies. We compare the weak emission–line galaxies and the BL Lacs in a sample of 57 flat–spectrum objects (Marchã et al. 1996), using high-frequency radio and non-thermal optical flux densities, spectral indices and polarization properties. We consider whether objects which are not 'traditional' BL Lacs – due to their larger emission line strengths, and larger Ca II spectral breaks – are simply starlight diluted BL Lacs. Their broad-band spectral properties are consistent with this interpretation, but their radio polarization may indicate more subtle effects. Comparison of the weak emission–line galaxies and the BL Lacs shows that, on average, the former have steeper spectra between 8 and 43 GHz, and are less polarized at 8.4 GHz. This is consistent with many of the weak–lined objects being at larger angles to the line of sight than the BL Lacs. In addition to this population, we indicate a number of the weak emission–line galaxies which may be 'hidden BL Lacs': relativistically boosted objects very close to the line of sight with an apparently weak AGN.

Key words: galaxies: active – galaxies: BL Lacertae objects: general – galaxies: jets – galaxies: nuclei – radio continuum: galaxies

1. Introduction

Explanations of different source properties as a manifestation of orientation dependent effects have been successful in both studies of high–powered radio galaxies and quasars, and in radio–weak Seyferts. Obscuration of the nuclear regions by a putative dusty disk at large angles to the line of sight is believed to turn Type I sources (Seyfert Is and quasars) into Type 2 sources (Seyfert 2s and narrow-line radio galaxies) (Scheuer 1987; Barthel 1989; Antonucci 1993). Viewing–angle dependent effects attributed to relativistic bulk flows (superluminal motion, rapid variability, core dominance, one-sided appearance) are also seen in the powerful radio sources (Urry & Padovani, 1995, and references therein)

Send offprint requests to: J. Dennett-Thorpe (jdt@astro.rug.nl)

The effects of orientation at intermediate radio luminosities remain much less clear (see Urry & Padovani 1995 for a review). It is now well accepted that BL Lacs are predominantly FRI radio sources seen at close angles to the line of sight. Many of their distinctive characteristics can be attributed to relativistic motion close to the line of sight: the FRI/BL Lac inner jets are believed to have γ between 2 and 20 (Urry & Padovani, 1995; Lara et al., 1997), and BL Lacs are thought to be those objects seen within $\sim 30^\circ$ to the line of sight (Urry & Padovani, 1995; Ghisellini et al., 1993). The role of obscuration at these intermediate luminosities however remains uncertain (see e.g. Falcke, Gopal-Krishna & Biermann, 1995; Jackson & Marchã, 1999; Chiaberge, Capetti & Celotti, 1999). Furthermore, many important questions remain unanswered or disputed: the relationship between the BL Lacs selected by different means (are the X-ray selected BL Lacs closer to the line of sight than the radio selected ones, or vice versa? or are they objects with underlying different energy distributions? (Fossati et al., 1997; Padovani & Giommi, 1995; Maraschi et al., 1986)); the frequency of BL Lacs which have FRII parents (Kollgaard et al., 1992; Stanghellini et al., 1997; Jackson & Wall, 1999).

In this paper we analyse the radio properties of a sample of flat–spectrum radio sources (Marchã et al., 1996). Such a population should contain a high fraction of sources at small angles to the line of sight. Indeed, Marchã et al. found a high fraction of BL Lacs and candidate BL Lacs, as well as both weak and strong emission–line objects. The canonical parent population of BL Lacs, the FRIs, are generally weak emission–line objects and so the weak emission–line objects in the sample could be objects which were somewhat further from our line of sight. (The relationship, if any, to the strong emission–line objects is less clear.)

Browne & Marchã (1993) suggested that objects which do not meet the generally used criteria for classification of an object as a BL Lac (EW$<$5Å, CaII break contrast $\leq$0.25; Stickel et al. 1991; Stocke et al. 1991) may still be BL Lacs, but whose identifying characteristics are diluted by starlight. Therefore new criteria were adopted by Marchã et al. (1996) [hereafter MBIS] to allow for this possible starlight dilution. Under these criteria, objects were classed as BL Lac candidates if they had CaII break contrasts lower than 0.4 and EWs that could be up to $\sim$

30 Å. As an extension of this idea, it is possible that some of the weak emission–line galaxies are not actually (substantially) further from the line of sight than the BL Lacs, but that they are 'hidden BL Lacs'. That is, their non-thermal emission at optical wavelengths was fainter than the identified BL Lacs, and therefore their nuclear emission is completely swamped by the starlight of the host galaxy. In this scenario the jet is still relativistic and beamed towards the observer at the same, or slightly greater, angles as occurs in BL Lacs.

In this paper we address:
(i) whether the BL Lac 'candidates' found by MBIS have broad band spectral properties consistent with their being bona-fide, but starlight diluted, BL Lacs.
(ii) the relationship of the BL Lacs with the weak emission line galaxies (WLRG), by comparison of their broad band spectral properties and core radio polarization. We analyse whether any of the WLRG are candidates for 'hidden' BL Lacs.

In a future paper, we use the results of this study and the radio morphologies to further analyse the relationship of the BL Lacs with the WLRG and, further, to investigate relationship of the broad emission–line galaxies (BLRG).

Sect. 3 records the observational parameters, Sect. 4 discusses the methods used in analysis of the data and presents some of the measured source parameters in tabular form. Sect. 5 considers these in the light of the spectral classification of the sources, the discussion of which is deferred to Sect. 6.

2. The sample

The sample is the 57 objects of MBIS. These objects satisfy the selection criteria $S_{5\rm GHz} > 200$mJy, $\delta > 20^\circ$ and $m_v < 17$. The Hubble relation for radio sources shows that these criteria will enable selection of an essentially complete redshift–limited subsample with z<0.1. Thus MBIS define a complete sample of 33 flat–spectrum objects with $S_{5\rm GHz} > 200$mJy at z<0.1. MBIS divide their sample into 6 categories: the known BL Lacs and new BL Lacs discovered by them which satisfy the Stocke et al. (1991) equivalent width–CaII break contrast criteria (EW<5 Å, contrast <0.25), the 'candidate BL Lacs', the weak emission–line galaxies, the strong emission–line objects (both broad– and narrow–lined), and two 'hybrid' objects which have properties intermediate between BL Lacs and quasars (Jackson & Marchã, 1999). There are also a few objects for which they were unable to obtain spectra and whose classification is therefore unknown.

We assign the class 'BL Lac' to those objects (both the 'known' and 'new' BL Lacs of MBIS) which fall within the Stocke et al. criteria. Those which fall outside this region, but within the extended criteria of MBIS, we classify as 'candidate BL Lacs' (although due to a change in definition of the contrast our classification of 'candidate' BL Lacs differs slightly from that used in MBIS – see Sect. 4.2). Thus Mrk 501 (B 1652+398) is classed as a 'candidate' BL Lac, on account of its EW(Hα) (MBIS). This object is already often classed as a BL Lac due to its extreme optical brightness, which makes it a subject of frequent study.

Table 1. The observational parameters

Oct 1997. VLA CnD array					
frequencies GHz		$\Delta\nu$ MHz	beam (")	ave. # visib.	rms mJy/bm
8.435	8.485	50	8	1200	0.25
14.965	14.915	50	3	2100	0.4
22.485	22.435	50	3	6500	0.6
43.315	43.365	50	1	3200	2

In this paper we are primarily interested in the categories of BL Lacs, candidate BL Lacs and weak emission line objects, although we will comment on the status of the strong emission line objects and hybrids, and for completeness include information on the objects of unknown spectral type.

3. Observations and data reduction

The observations were taken with the NRAO VLA CnD array on 29 September and 5, 18 and 27 October 1997. 43 GHz receivers are only available on 13 antennae: we therefore observed 22 GHz and 43 GHz in one subarray, and 8 and 15 GHz simultaneously in the other subarray. On-line integration times were 3.3s. Observing parameters and typical rms noise levels are shown in Table 1. Fast switching was used at 43 GHz where this was beneficial (the existence of a nearby bright good calibrator at this frequency), but in general this was not done: the phase stability in the relatively compact array was sufficient, and moreover the relatively strong, point-like structure of the sources themselves allowed for most sources to be self-calibrated. Absolute flux density and polarization position angle calibration were done with reference to 3C 286. Due to failure of the telescope, three sources have no data at any frequency (B 1646+499, B 1652+398 and B 1703+223), and one only at 8 GHz (B 1658+302).

4. Data analysis

4.1. The high frequency radio observations

The flux densities were measured using the AIPS image and (u,v)–plane fitting tasks IMFIT and UVFIT. At these resolutions, all the sources are dominated by a single component at 8 GHz and higher. It was therefore found that a good fit was obtained to all sources with a single Gaussian and a zero-level offset with slope, if the fit was restricted to the region ~ 3 times FWHM of the restoring beam. The values from IMFIT obtained in this manner were used as the flux densities of the core. The error was estimated using the difference between this and those obtained by UVFIT. At 8 GHz the 'fitting' error calculated in this manner is very small. At 43 GHz the UVFIT and IMFIT tasks sometimes yield different results due to the very low signal-to-noise ratio on any given visibility. The total quoted error also includes a 3% calibration error.

We fitted a power–law spectrum to all the high frequency data ($S \propto \nu^{-\alpha}$), using a χ^2 fit, taking account of the errors on the

derived flux densities. Only one source (B 1404+286, a known GPS) had a (down-curving) spectra clearly inconsistent with the straight line fit. B 1404+286 was included in the sample of MBIS as it is a serendipitously flat spectrum source between 1.4 and 5 GHz, as its spectral peak falls near these frequencies. The error on the spectral fits is simply the weighted χ^2. Examples of the spectra and the fits are shown in fig 1. The core polarized flux density was calculated from similar fits to Ricean corrected polarized intensity maps. The 8.4 GHz flux densities, spectral indices between 8.4 and 43 GHz and percentage polarization measured at 8.4 GHz, with accompanying errors, are presented in Columns 3 to 8 of Table 2, which presents the observational results for all sources.

4.2. The non-thermal contribution to the optical flux densities

The observed optical continuum is the sum of the contribution from the host galaxy ($S_{\rm o}^{\rm G}$) and that arising from the AGN ($S_{\rm o}^{\rm AGN}$). As the objective is to establish the broad–band properties of a sample of AGNs, it is important that the AGN contribution alone is considered.

The optical spectrum of early–type galaxies shows a prominent flux depression shortward of 4000 Å which is referred to as the Ca II break or the 4000 Å break. The strength of this break is quantified by the break contrast, C:

$$C = \frac{S_\nu^+ - S_\nu^-}{S_\nu^+} \quad (1)$$

where $S_\nu^{-,+}$ are the flux densities at wavelengths respectively longer and shorter than the Ca II break.

Dressler & Shectman (1987) studied a large sample of galaxies and found that ellipticals had a mean break contrast of $\langle {\rm C}^{\rm G} \rangle$ = 0.49. Inspection of their data showed that less than 5% of early-type galaxies have break contrasts below 0.4. It is therefore a reasonable assumption that an elliptical galaxy with C $\leq$ 0.4 has an extra source of continuum which reduces the strength of the Ca II break. In other words, if the measured break contrast is found to be below 0.4, there is good statistical evidence to assume that it is due to an extra source of continuum, in particular, a non-thermal source due to the AGN. We therefore calculate the non-thermal contribution from the measured break contrast and total optical flux, according to:

$$S_{\rm o}^{\rm AGN} = \frac{\langle C^{\rm G} \rangle - C}{\langle C^{\rm G} \rangle} S_{\rm o}. \quad (2)$$

There is no reason why objects showing break contrasts larger than 0.4 should not hold extra sources of continuum, but these will not be detected via the measurement of the contrast (i.e. they are the 'hidden BL Lacs').

It should be noted that the above equation is valid only for sources in which the line contribution to the optical spectrum is negligible, and where C $\leq$ 0.4. For those sources where there is either a significant emission line contribution or C$>$ 0.4, the estimated optical non-thermal contribution is likely to be overestimated. Furthermore, any non-thermal optical contribution

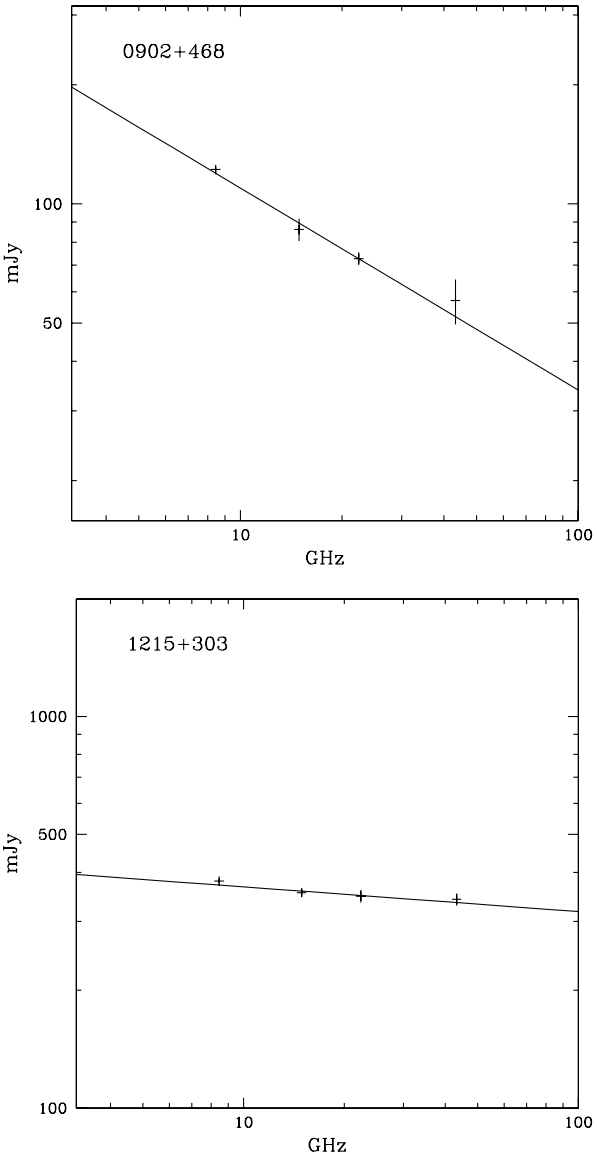

Fig. 1. Examples of the spectra and fits obtained: a falling spectrum WLRG, B0902+468, and BL Lac B1215+303 with a flat spectrum.

for those sources with C$>$0.5 cannot be estimated in this manner. In these latter cases, we assigned a break contrast of 0.49, and obtained an upper limit of $S_{\rm o}^{\rm AGN}$. Finally, we mention that the $S_{\rm o}$ should be measured close to the rest-frame wavelength of the Ca II break (4000 Å). We measured the flux density at a rest–frame wavelength of 5500 Å, in order to be consistent with the wavelength usually considered when determining the broad–band spectral indices. We will show that our results are not dependent on this choice.

We use Eq. 2 to estimate the AGN contribution to the optical flux for the sources for which there is a break contrast given in MBIS. For sources without measured break contrasts (the BL Lacs), either the spectra of MBIS were used to determine the non-thermal emission, or where these were not taken (due to the status of an object as a known BL Lac), the V band magnitudes from the literature were used to esti-

Table 2. The source properties: 8 – 43 GHz and 5000 Å

Source	type	contrast	S(8GHz) (mJy)	+/-	α(8.4–43GHz)	+/-	%P(8GHz)	S_o(5500 Å) (mJy)	S_o^{AGN}(5500 Å) (mJy)	other name
B 0035+227	WE	0.57	181	5	0.88	0.06	<0.81	0.30	<0.01	
B 0046+316	NE	0.35	260	8	0.38	0.05	2.22	1.32	0.40	Mrk348
B 0055+300	WE	0.56	798	24	0.06	0.04	<0.18	3.96	<0.08	NGC315
B 0109+224	KB	0	1472	44	-0.46	0.04	1.62	2.0	2.0	
B 0116+319	WE	0.56	1107	33	0.75	0.05	0.22	0.60	<0.01	4C31.04
B 0125+487	HY	0.38	177	5	-0.15	0.05	3.48	0.31	0.07	
B 0149+710	WE	0.46	457	14	0.03	0.03	2.67	0.63	0.05	
B 0210+515	KB	0.26	182	6	0.28	0.04	3.29	0.93	0.44	
B 0251+393	BE	0.00	456	14	0.13	0.04	1.67	0.30	0.30	
B 0309+411	BE	0.25	458	14	-0.04	0.05	0.92	0.22	0.11	
B 0316+413	BE	–	22531	677	0.41	0.03	0.25	–	–	3C84/PerA
B 0321+340	NE	0.00	493	15	0.38	0.04	4.53	0.97	0.97	
B 0651+410	WE	0.55	288	9	0.17	0.04	<0.43	2.01	<0.04	
B 0651+428	CB	0.26	156	5	0.25	0.04	1.31	0.36	0.18	
B 0716+714	KB	0.00	719	22	0.01	0.06	5.23	123.00	123.00	
B 0729+562	WE	0.61	123	4	0.75	0.07	<1.02	1.00	<0.02	
B 0733+597	WE	0.58	185	6	0.34	0.06	<0.62	1.62	<0.03	
B 0806+350	KB	0.25	108	3	0.44	0.06	2.98	0.66	0.32	
B 0848+686	WE	0.54	44	3	0.13	0.16	2.54	2.53	<0.05	
B 0902+468	WE	0.54	122	4	0.51	0.05	<0.99	0.71	<0.01	
B 0912+297	KB	0.07	178	7	0.39	0.03	2.69	1.58	1.36	
B 1055+567	CB	0.08	196	6	-0.06	0.03	1.31	3.26	2.73	
B 1101+384	KB	0.06	656	20	0.17	0.03	2.37	60.90	54.20	Mrk421
B 1123+203	CB	0.11	428	14	0.24	0.03	<0.28	0.86	0.68	
B 1133+704	CB	–	147	5	-0.01	0.03	3.27	–	–	Mrk180
B 1144+352	WE	0.51	372	11	0.29	0.03	0.44	1.70	<0.03	
B 1146+596	WE	0.56	416	12	0.33	0.05	<0.31	7.33	<0.15	
B 1147+245	KB	0	770	27	0.19	0.03	1.38	1.51	1.51	
B 1215+303	KB	0	380	11	0.06	0.03	4.16	1.64	1.64	ON235
B 1217+295	WE	–	132	4	0.65	0.07	0.65	–	–	NGC4278
B 1219+285	KB	0	696	21	0.23	0.05	3.64	1.02	1.02	WCom
B 1241+735	WE	0.49	139	5	0.15	0.03	8.02	1.25	0.01	
B 1245+676	WE	0.56	136	4	0.56	0.05	<1.02	0.56	<0.01	
B 1254+571	BE	–	245	7	0.79	0.04	<0.50	–	–	Mrk231
B 1404+286	BE	0.25	1932	59	0.99⋆	0.05	0.11	1.72	0.86	OQ208
B 1418+546	KB	0.18	616	18	-0.07	0.03	3.01	2.06	1.33	OQ530
B 1421+511	BE	0.00	132	4	0.01	0.04	1.06	0.51	0.51	
B 1424+240	KB	0.00	254	8	0.20	0.04	2.63	4.28	4.28	
B 1532+236	NE	–	148	5	1.03	0.12	<0.84	–	–	Arp220
B 1551+239	WE	0.47	132	5	-0.07	0.05	<0.88	0.46	0.03	
B 1558+595	WE	0.57	109	4	0.89	0.13	<1.06	2.03	<0.04	
B 1645+292	KB	0.34	74	3	0.58	0.15	4.68	0.35	0.12	
B 1646+499	HY	0.37	–	–	–	–	–	0.76	0.20	
B 1652+398	CB	0.18	–	–	–	–	–	11.80	7.47	Mrk501
B 1658+302	WE	0.54	86	2	–	–	<1.97	1.18	<0.02	
B 1703+223	WE	0.53	–	–	–	–	–	0.81	<0.02	
B 1744+260	CB	0.36	266	8	0.08	0.04	1.55	0.22	0.06	
B 1755+626	WE	0.59	150	5	0.17	0.03	1.62	2.35	<0.05	NGC6521
B 1807+698	KB	0.15	1501	45	-0.07	0.04	3.11	4.37	3.09	3C371
B 1959+650	KB	0.10	254	8	-0.12	0.03	1.61	1.45	1.16	
B 2116+818	BE	–	135	6	-0.35	0.04	<1.09	0.96	0.96	
B 2202+363	WE	0.55	121	4	-0.12	0.03	<1.26	0.72	<0.01	
B 2214+201	UK	–	109	8	0.59	0.11	9.54	–	–	
B 2217+259	BE	0.35	208	6	-0.08	0.03	<0.80	0.52	0.15	
B 2319+317	UK	–	623	19	0.06	0.03	0.19	–	–	
B 2320+203	WE	0.53	151	6	0.21	0.04	1.41	1.59	<0.03	
B 2337+268	UK	–	100	6	0.20	0.05	2.89	–	–	NGC7728

Spectral types (outlined in Sect. 4.2): KB and CB are known and candidate BL Lacs respectively. BE and NE are strong emission line objects with broad and narrow lines respectively. WE are objects with weak emission lines and a spectrum dominated by stellar light. HY are hybrids, and UK are of unknown spectral type.

⋆ down-curving spectrum not well fit by straight line.

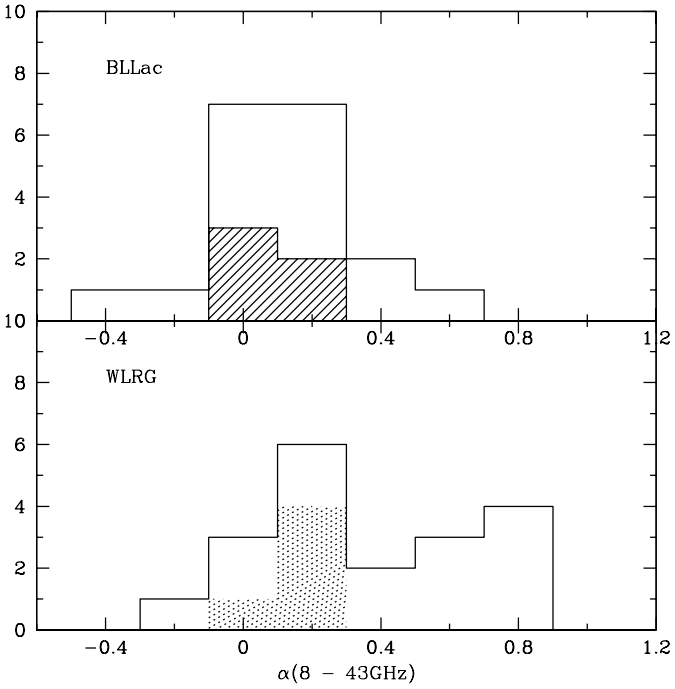

Fig. 2. Histograms of the high frequency spectral indices of (top panel) the BL Lacs and candidates; candidate BL Lacs hatched and (bottom panel) weak emission line galaxies. The shaded region in the bottom panel corresponds to potentially 'hidden' BL Lacs (see Sect. 6.2.)

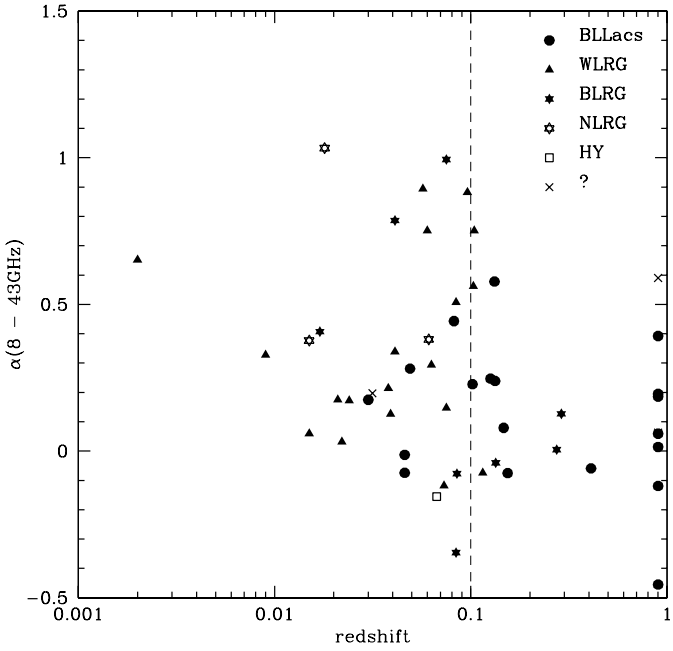

Fig. 3. High frequency radio spectral index as a function of redshift for the different classes. The dotted line indicates the redshift limit corresponding to the 'complete sample' of MBIS. Objects of unknown redshift have been placed arbitrarily at z=1

Table 3. Mean properties of classes of objects

category	BL Lac	CBL Lac	WLRG	BLRG
$S_{8\rm GHz}(mJy)$	561±461	239±116	272±269	2950±7364
α^8_{43}	0.13±0.27	0.10±0.14	0.35±0.32	0.22±0.43
$\alpha^{\rm radio}_{\rm opt*}$	0.47±0.13	0.58±0.15	–	–
%P (8GHz)	3.0±1.1	1.5±1.0	<1.4±1.7	0.8±0.5

The mean percentage polarization of the WLRG at 8.4 GHz is calculated using the upper limits

mate the non-thermal optical flux density (assuming $\alpha_{\rm opt}$ =0). These were: B 0109+224 (Puschell & Stein, 1980), B 1147+245, B 1215+303 and B 1219+285 (Tapia et al., 1976). A spectrum from the literature was used for B 2116+81 (Stickel et al., 1993).

The values of the contrast and optical flux densities are tabulated in Table 2. The contrast values given here are slightly different from those in MBIS since the latter were calculated using S_λ in Eq. 1, instead of the definition used here (S_ν). The new values (consistent with Dressler & Shectman (1987)) result in contrasts >0.4 for the sources B 0149+710, B 1144+352, B 1551+239, and B 1703+223. In what follows we no longer classify these sources as 'candidate' BL Lacs as in MBIS, but comment on them individually where this is thought appropriate. We note however, that this leaves only candidate objects very close to the Stocke et al. criteria in EW-contrast space, and B 1744+260 (which lies closer to the 'hybrids' B 0125+487 and B 1646+499.) The new classifications are in Column 2 of Table 2.

5. Results

5.1. High frequency radio spectra

Firstly we consider high frequency radio spectra of the BL Lacs and the 'candidate' BL Lacs ($S\propto \nu^{-\alpha}$). As can be seen on the top panel of Fig. 2, the candidate BL Lacs (hatched) are indistinguishable from the BL Lacs (white) by their high frequency radio spectra. (A Kolmogorov–Smirnov (K-S) test rejects the hypothesis that they are drawn from the same population only at the 13% level.) This is in marked contrast to the weak emission–line galaxies: a comparison of the top and bottom panels shows that the WLRG have a steeper radio spectra than the BL Lacs. This is confirmed by a K-S test: the hypothesis that the WLRG and BL Lacs (including candidate BL Lacs) are drawn from the same population is rejected at the 88% level.

As the BL Lacs are generally at higher redshifts than the WLRG (although there are 7 BL Lacs with unknown redshifts), the intrinsic rest–frame difference in the spectra of the two classes is likely, if anything, to be greater than the difference observed. However, Fig. 3 shows there is no dependence of the spectral index α^8_{43} on redshift for any of the different classes.

The BLRG and the BL Lacs have a similar distributions of α^8_{43}. The one hybrid which was successfully observed, B 0125+487, has a rising spectrum in this frequency range.

5.2. Radio to optical spectra

The radio–optical non-thermal spectral index can be used to assess the similarity of the 'candidate' BL Lacs and the known BL Lacs over a large frequency range. The top panel of Fig. 4

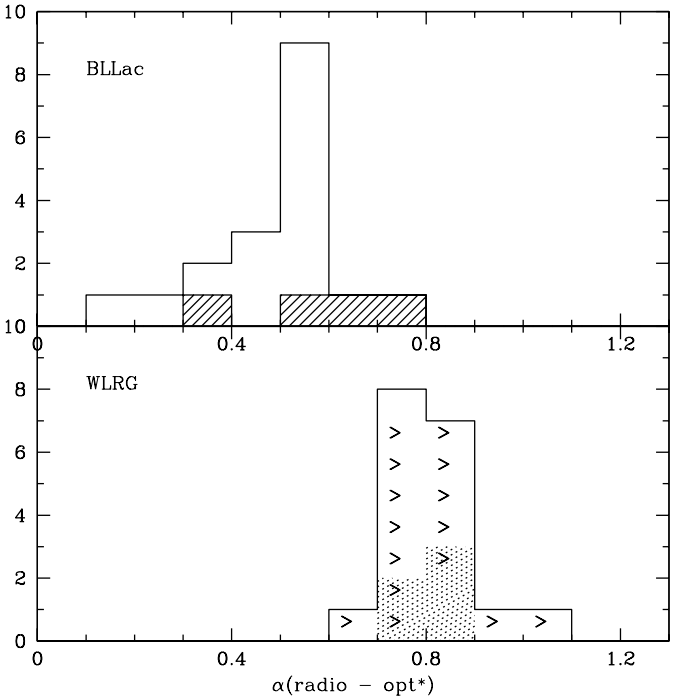

Fig. 4. Histograms of the radio to non-thermal optical spectral indices of (top panel) the BL Lacs and candidates; candidate BL Lacs hatched and (bottom panel) weak emission line galaxies. The shaded region as for Fig. 2.

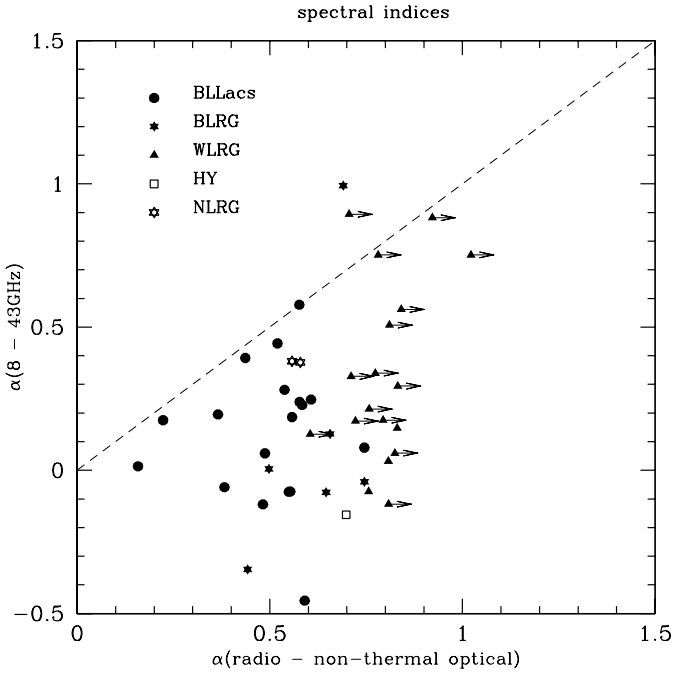

Fig. 5. Non-thermal spectral indices. The optical flux densities used are only the non-thermal contribution at 5500 Å, as explained in the text.

shows the radio–optical spectra of the BL Lacs and (hatched) candidates. For the known BL Lacs the mean spectral index $\bar{\alpha}^{\rm rad}_{\rm opt*} = 0.47 \pm 0.13$, and for the candidates $\bar{\alpha}^{\rm rad}_{\rm opt*} = 0.58 \pm 0.15$, where opt$*$ refers to the non-thermal contribution to the optical flux. That they are drawn from the same population is rejected by a K-S test with a probability of 88%. A second estimate of the non-thermal optical flux densities from S. Anton (priv. comm.), combined with our data calculated from literature values, gives spectral indices of 0.50±0.14 for the BL Lacs and 0.63±0.17 for the candidates. This second estimate is not calculated at 5500 Å in the rest-frame, but over wavelengths selected to be free of emission lines nearer the 4000 Å break. Using these values, the same parent population is rejected at the 95% level.

Thus we see that the spectra of the candidate BL Lacs show some marginal indication of steepening more rapidly than those of the known BL Lacs in the sample. The candidates and known BL Lacs do not show significantly different distributions in 8.4 GHz or optical (5500 Å) flux densities: either the total or the AGN component.

The radio–optical non-thermal spectral index is less useful for comparison of the BL Lacs with the WLRG because the measurement of the AGN component at 5500 Å is necessarily dominated by the error in the uncertainty of the underlying stellar spectrum. However a clear difference between the populations can be seen in Figs. 4 and 5. In these plots the points marked with lower limits refer to a calculation of the non-thermal contribution as outlined in Sect. 4.2. Using these upper limits as measurements, we can reject the possibility that the samples are the same at greater than the 99.99% level.

The BLRG and the BL Lacs show similar distributions of non-thermal optical to radio spectral indices, $\alpha^{\rm rad}_{\rm opt*}$, illustrated in Fig. 5.

5.3. Radio polarization

Our new observations of radio polarization at 8 GHz are in general agreement with those in MBIS, although our upper limits tend to be more conservative. (The polarization observations quoted in MBIS were taken from observations done in 1990–91 (Patnaik et al., 1992; Wilkinson et al., 1998).) Three sources have markedly different degrees of polarizations between the two sets of observations: these are B 1144+352 and B 1123+203 (decrease) and WLRG B 1241+735 (increase). These differences are commented on before discussing the sample as a whole.

The peculiar source B 1144+352, as has already been noted, is known as a GPS source (Snellen et al., 1995) and VLBI maps show a $\sim$ 50 pc double structure (Henstock et al., 1995) with components superluminally expanding (Giovannini et al., 1999), and known to be variable (see Schoenmakers et al. 1999). Schoenmakers et al. (1999) argue convincingly that this is the core of a mega-parsec sized giant radio galaxy. The radio polarization drop may be real, as the source was apparently near its maximum flux density at the time of the first observations (Schoenmakers et al. Fig. 7). Alternatively the 2σ detection may have been erroneous, associated with a component other than the core, or the lower resolution of the observations presented here results in beam depolarization.

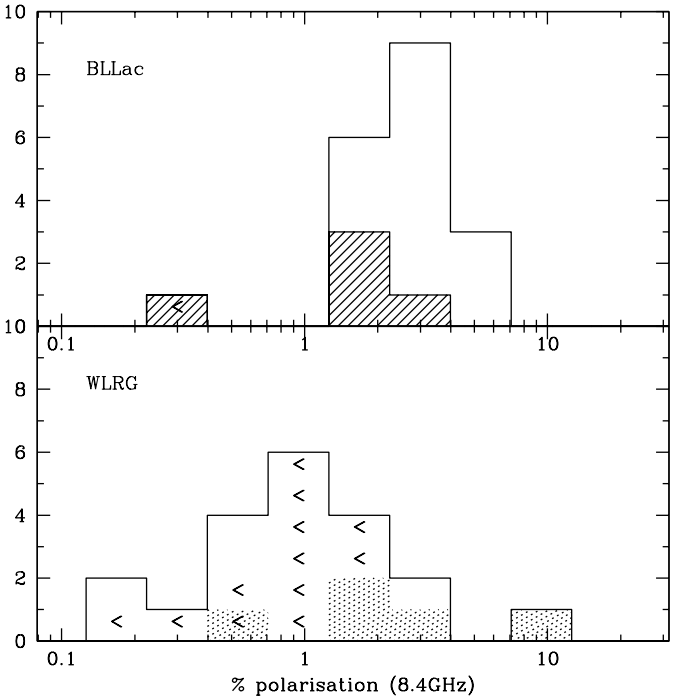

Fig. 6. Radio polarization at 8.4 GHz, as a function of spectral class.

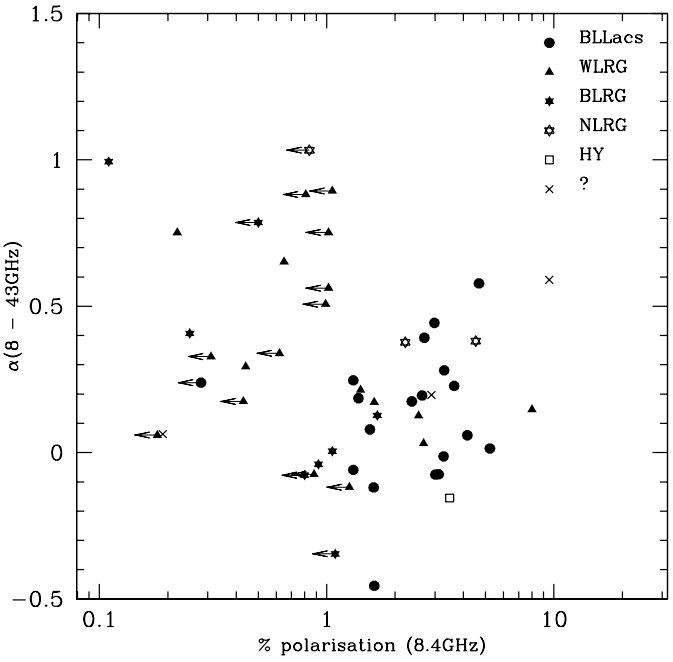

Fig. 7. Radio polarization at 8.4 GHz, and high frequency radio spectral index. Crosses refer to objects of unknown spectral type. Arrows are upper limits set at $2.5 \times (\sigma Q + \sigma U)$, where σQ and σU are the noise on the Stokes Q and U maps respectively.

The candidate BL Lac B 1123+203 (PGC 035156) has shown extreme optical variability over a period of two decades, dominated by long-term changes (Pica et al., 1988), and has apparently also suffered a polarization drop in the 6 years since the previous 8 GHz measurements.

B 1241+735 shows very high radio polarization in these observations: a remarkable 9% for an object classified as a WLRG. Augusto et al. (1998) show this source to have a core-jet structure in MERLIN observations.

Another source with high percentage of radio core polarization is the 'red stellar' (MBIS) object of unknown spectral type B 2214+201. This unusual object was the most polarized object at both epochs and may be a star, perhaps with an extragalactic radio source along the same line of sight.

In general we reproduce the radio polarization results of MBIS: the BL Lacs are significantly more polarized at 8 GHz than the WLRG (Fig. 6). Based on their percentage polarization at 8.4 GHz, the probability that BL Lacs and WLRG are drawn from the same population is rejected at 99.98% level (using upper limits as detections). It can also be seen in Fig. 6 that the candidate BL Lacs have a lower polarization than the known BL Lacs. The K-S test on the BL Lacs and candidates shows only a 2% chance that they are drawn from the same population. Even with the exclusion of the source B 1123+203 which showed little polarization in these observations, the populations remain distinct, with only a 6% chance that they are from the same population.

We also reveal a new effect: the weak emission line objects with radio polarization $> 1\%$ also have flat high frequency radio spectra. Fig. 7 shows the 8 GHz polarization and high frequency spectral index for all the objects. The known WLRG in this group of flat spectrum, high polarization sources are: B 0149+710, B 0848+686, B 1241+735, B 1755+626 and B 2320+203.

5.4. Variability

Clear evidence of variability is seen in a number of the BL Lacs and BL Lac candidates. Studies of radio variability with the available data of this sample are hampered by the different telescopes used at different epochs. Nonetheless it is seen that a comparatively large number of these sources show large differences in flux densities between the 87GB (Gregory & Condon, 1991) and GB6 (Gregory et al., 1996) surveys at 4.85 GHz, and/or the Green Bank (White & Becker, 1992), NVSS (Condon et al., 1998) and FIRST (White et al., 1997) surveys at 1.4 GHz. Indeed, the variability of BL Lacs at radio wavelengths is well-known, and the subject of a number of ongoing monitoring campaigns (see e.g. Aller et al. 1999) which include a number of these objects.

Three other sources show evidence for variability at 1.4 GHz as the VLA B array flux density (as measured by FIRST or own observations (forthcoming paper)) is greater than the VLA D array flux density from NVSS. The VLA B array is likely to resolve out source structure, and so we could explain a lower B array flux density without recourse to variability, but not a higher B array flux density. The non-BL Lac sources which fall in this latter category are: two WLRGs B 0729+562, B 2202+363 and one object of unknown spectral type B 2319+317.

6. Discussion

6.1. The status of the 'candidate' BL Lacs

As the objects classified as 'candidate BL Lacs' occupy a different region on the contrast-EW plane than the other BL Lacs, we first address whether the data are consistent with them being the same type of object: that is, are they otherwise identical to the other BL Lacs? If they have statistically different properties, are these differences explicable if we assume that the candidate BL Lacs are simply either slightly further from our line of sight, or intrinsically weaker (relative to their hosts)? In either of these cases the hypothesis of MBIS that they are starlight diluted BL Lacs then holds.

It was shown in Sect. 5 that the spectral indices in the 8–43 GHz regime were indistinguishable between the BL Lacs and the candidate BL Lacs. It was also shown that there was a marginal difference in the radio–optical non-thermal spectral indices, and that the candidate BL Lacs were less polarized at 8.4 GHz. The first piece of evidence is clearly consistent with the notion of starlight diluted BL Lacs, particularly striking as they differed from the population of WLRG. However, the remaining two differences require some consideration, which is given below.

First we consider the marginal difference in $\alpha^{\rm rad}_{\rm opt*}$. In a sample such as this which is selected with two flux density limits (i.e. both in the radio and in the optical), we must consider the effects of this selection on the properties of our sample. The optical magnitude limit implies that for objects which are dominated by starlight there will be a smaller flux density attributable to the non-thermal emission at 5500 Å: as there is no difference in the total optical emission from the two classes of objects, we expect that the optical emission due to the non-thermal AGN is weaker in the objects classified as candidate BL Lacs. Indeed, this is so, but the genuine BL Lacs are also brighter in the radio, which makes it unclear as to whether the difference in spectra is due solely to this selection effect. Therefore no firm conclusions can be based upon the marginal difference: the difference could arise simply due to selection effects, or may reflect a real difference, or simply small number statistics (there are only 4 candidate BL Lacs with calculated $\alpha^{\rm rad}_{\rm opt*}$).

The lower fractional polarization of the candidate BL Lacs cannot, however, be attributed to a selection effect. Simple theories of BL Lac emission with a synchrotron origin for both the radio and the optical emission could be used to deduce constraints on the intrinsic conditions or angle to the line-of-sight in these objects, but small number statistics constrain us to discuss this only in qualitative terms. One possibility is that the candidate BL Lacs have lower radio polarization because this sample is at slightly larger angle to the line of sight than the other BL Lacs. In this way they are objects which are more 'starlight diluted' principally because they are less Doppler boosted due to a line of sight effect, rather than due to the relative intrinsic weakness of the source.

One potential problem with this idea is that, according to the 'accelerating jet' model (Marscher 1980; Ghisellini & Maraschi 1989) for objects dominated by this accelerating region of the jet, the spectrum typically steepens as objects move into the line of sight. This is the opposite of what, if anything, is observed as we move from the BL Lacs to the candidates, although as we have pointed out, there is a problem of a selection effect here.

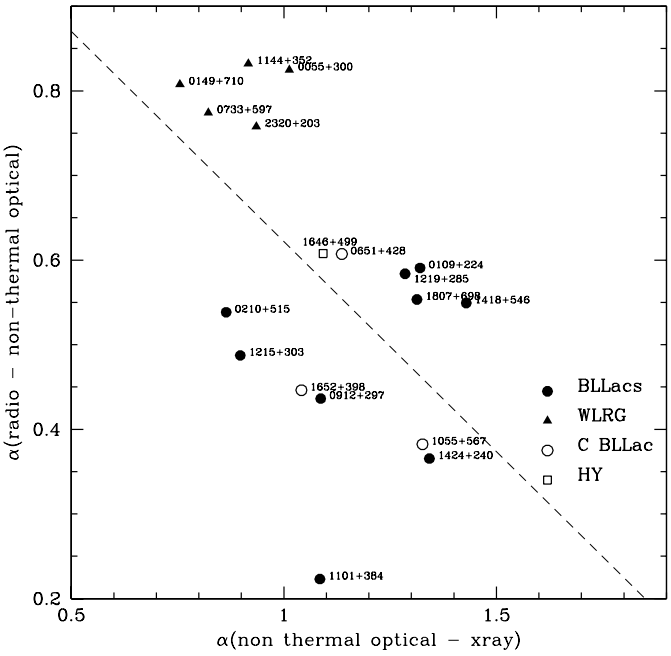

Fig. 8. The radio-optical-xray of the objects in the sample. The Radio flux densities are those tabulated in Table 2, except for B 1646+499 and B 1652+398 for which we use the 8.4 GHz flux densities of Patnaik et al. (1992). The X-ray flux densities are from the ROSAT All-Sky Survey. Only sources detected in this survey are plotted. We plot BL Lacs and candidates (CBL Lacs) as well as the WLRG and the detected hybrid B 1646+499. The dashed line corresponds to the 'dividing line' between HBLs and LBLs (after Padovani & Giommi 1995)

On the other hand, intrinsically weaker objects may have different synchrotron turn-over frequencies (or maximum particle energies). Ghisellini (1997) suggests that the difference in blazar spectral energy distributions could be explicable by differing amounts of radiative cooling due to electrons. These electrons could be from the BLR. In this scheme the candidate BL Lacs, with stronger emission lines might suffer stronger radiative cooling, and therefore be expected to have a steeper $\alpha^{\rm rad}_{\rm opt*}$. This could only explain the difference in polarization properties if this was due to depolarization in a medium associated with the emission line region.

The discussion here has parallels to the debate over the relation between X-ray– and radio–selected BL Lacs (XBLs and RBLs) or, complimentarily, high– and low–energy cut-off BL Lacs (HBLs and LBLs) (see e.g. Maraschi et al. 1986; Padovani & Giommi 1995): are the differences intrinsic or due to a line of sight difference? The accelerating jet model has had a number of difficulties in reproducing the characteristics of the XBL and RBL populations, and recent work has focussed either on intrinsic physical differences (Padovani & Giommi 1995) or on a combination of both (Georganopoulos & Marscher 1998).

Indeed these parallel discussions may be no coincidence – it could be that our candidate BL Lacs are 'XBL-like': Mrk501 has been called a 'candidate' by us, and was called XBL-like by Padovani & Giommi (1995). In this light we plot (Fig. 8) the $\alpha_{\rm o}^{\rm r} - \alpha_{\rm x}^{\rm o}$ plane, which has divided these populations until the more recent discovery of an 'intermediate' population (Perlman et al., 1998; Laurent-Muehleisen et al., 1999). We plot the non-thermal contribution to the optical flux density only (the plots in the literature use the entire optical flux density). This has the effect of moving the points left and up, although for the BL Lacs this effect is negligible. By comparison with Stocke et al. (1985) we see that all our BL Lacs fall somewhat nearer the 'dividing line' (illustrated Fig. 8) than either the complete 1 Jy and EMSS samples, which lie to the top right and bottom left respectively. Furthermore, the candidates, as well as the other BL Lacs, appear both RBL-like and XBL-like by this measure.

Our spectral results for the BL Lac population as a whole are consistent with those of Gear et al. (1994), who find for a subset of the Stickel et al. (1991) sample of BL Lacs, flat or rising spectra in the range 5 to 37 GHz ($\alpha = -0.04 \pm 0.20$), and falling spectra in the range 150 to 375 GHz ($\alpha = 0.48 \pm 0.22$). They also find, for the cases they have data, that the 90 GHz points are consistent with a single power law from 90 GHz to the millimeter regime. Bloom et al. (1994) also find falling spectra in the millimeter and sub-millimeter regime. These studies concluded that the spectral break for radio-selected BL Lac objects must lie in the range 10 to 100 GHz. For our sample we find flat or slightly falling spectra, with some examples of rising spectra in the range 8 to 43 GHz. Our observations are generally well fit by a single power-law, implying that for our objects the break must lie > 22 GHz (The 43 GHz points not having high enough signal to noise to rule out the start of a break in the spectra), or that the spectral break is not sharp (so would be undetected over such a small frequency range). The simplest interpretation is that this sample of somewhat fainter radio-selected BL Lacs has a gradual spectral turn-over at around the same frequencies (10–100 GHz) as the more powerful Stickel et al. ('1 Jy') sample.

We therefore conclude that the results can be explained by the hypothesis that the candidate BL Lacs are starlight diluted BL Lacs. The fact that the candidate BL Lacs are indistinguishable from the BL Lacs in the high frequency radio regime, with flat spectra extending out to 43 GHz, indicates that the candidate BL Lacs are still highly Doppler boosted. If the lower radio polarization of the candidate BL Lacs is explained by requiring the candidate BL Lacs to be slightly further from the line of sight than the other BL Lacs, the marginal difference in $\alpha_{\rm opt*}^{\rm rad}$ may reflect a selection effect.

6.2. The relationship of the WLRG and BL Lacs

We wish to address whether the WLRG are consistent with being the parent population of the BL Lacs: that is BL Lacs away from the line of sight, and, further, whether there is any indication that any of the objects in this class are 'hidden' BL Lacs: that is they are oriented at similar angles as the BL Lacs, but that the starlight contribution from their hosts swamps the characteristic non-thermal emission at optical wavelengths.

Unlike the situation for the BL Lacs themselves we cannot assume that the detected emission of the WLRG comes from jet-like structures. Augusto et al. (1998) presented VLBI observations which contained a number of the sources in this sample, and find the WLRGs B 0116+319 to be a CSO, and B 1241+735 to be a core–jet.

The mean 8–43 GHz spectral index is steeper for the WLRG than the BL Lacs. This is consistent with both emission from more extended regions and jet emission at larger angles to the line of sight, if the jet is no longer dominated by an accelerating inner jet. In the latter case this arises as the break in the spectrum (in BL Lacs at a few tens of GHz) is not Doppler shifted to such high frequencies.

At centimeter wavelengths with the resolution of the observations presented here, detailed interpretation of the polarization properties of the sample are not possible, as the effects of Faraday rotation and depolarization and jet bending complicate the interpretation. However the results are consistent with the canonical jet-in-shock model (e.g. Blandford & Konigl, 1979) If we consider the emission detected in the WLRG to be jet material, the comparatively unpolarized cores of the WLRG in comparison to the BL Lacs could arise either by Faraday depolarization by a surrounding dense magneto-ionic medium (e.g. torus) or by the dominance of a single Doppler–boosted shock structure in the BL Lacs. If the polarized emission comes from a variety of structures, or from the general jet material, we must favour Faraday depolarization of the WLRG to explain the difference in polarization properties. A further possibility is that the emission detected in the WLRG is not parsec-scale jet material as is it is for the BL Lacs: indeed, as mentioned above, the WLRG contain a number of known compact symmetric objects. The emission from these objects come from a variety of structures, including hotspots and any lobes, and in these cases the lack of polarization is most likely to be caused by beam depolarization.

Using the Rosat All-Sky Survey and the data presented in this paper, we suggest the following 5 sources contain AGN very close to the line of sight:

B 0149+710 has a RASS detection, high $\%{\rm P}_{\rm radio}$ and flat α_{43}^{8}; it has a relatively low Ca II break contrast, and was considered a candidate BL Lac in MBIS (see Sect. 4.2)

B 1144+352 too was considered a candidate BL Lac in MBIS, and has a RASS detection, as well as observed superluminal motion (Giovannini et al. 1999);

B 1241+735 is a core-jet source (Augusto et al. 1998) has a very high $\%{\rm P}_{\rm radio}$ and flat α_{43}^{8}

B 1755+626 has a high $\%{\rm P}_{\rm radio}$ and flat α_{43}^{8}

B 2320+203 has a RASS detection and a high $\%{\rm P}_{\rm radio}$ and flat α_{43}^{8}

These sources are potentially 'hidden' BL Lacs: those which are not detected by the measurement of the Ca II break, because their non-thermal continuum is swamped by starlight. These sources are shaded in the lower panels of Figs. 2, 4 and 6. These

sources have similar $\alpha_{\rm x}^{\rm o}$ to the BL Lacs, but steeper radio to optical spectra.

The other two RASS detections, namely B 0055+300 and B 0733+597 are also candidates of beamed AGN. B 0055+300 (NGC315) is a giant FRI, with an asymmetric two-sided jet and prominent core (the reason the source was included in the 200mJy sample). Due to the core brightness Venturi et al. (1993) argued the jet was highly relativistic. VLBI observations (Cotton et al. 1999) indicate Doppler favoritism as the cause of the brightness asymmetry on small scale and argue the jet is aligned at 35° to the line of sight. B 0733+597 shows a core-jet structure with a faint counter-jet to the south on VLBI scales (Taylor et al. 1994).

One hybrid (B 1646+499) was detected in the RASS, but unfortunately we have no high frequency radio data for this source. However in MBIS it was relatively strongly polarized at 8.4 GHz (1%). The other hybrid (B 0125+487) was also strongly polarized at 8.4 GHz (1.9% in MBIS, 3.4% here) and had a slightly rising α_8^{43} spectrum.

From the steep α_{43}^8, we suggest that B 0035+227, B 0116+319, B 1217+295 and B 1558+595 are likely not to be highly boosted objects, and may, like B 0116+319, turn out to be CSOs. B 0729+562 is intriguing because it too has a steep α_{43}^8, but has apparently shown variations at 1.4 GHz.

In summary, the steeper α_{43}^8 and lower radio polarizations of the WLRG as a population as a whole when compared to the BL Lacs can be explained if the WLRG are, on average, at larger angles to the line of sight. The fact that WLRG with radio polarization $> 1\%$ were found to have flatter α_{43}^8, can therefore be interpreted as identifying a sub-sample of WLRG closest to the line of sight. The high incidence of X-ray detections in this sub-sample supports this claim. We suggest that around a quarter of the WLRG in the sample are these 'hidden' BL Lacs. A similar number of sources may well turn out to be compact objects which are not highly relativistically boosted, but whose spectra is relatively flat at 1.4–5 GHz, as synchrotron losses do not yet dominate the sources. These WLRG may not be so directly related to the BL Lacs in the sample, and this should be borne in mind in further statistical studies. The remaining half of the sources we speculate to be predominantly core-dominated FRI-like sources, but which are not so close to the line of sight to be considered 'hidden BL Lacs'.

7. Conclusions

We have shown that the radio and radio–optical spectra are consistent with the 'candidate' BL Lacs of MBIS (revised definition in Sect. 4.2 for compatibility with other workers) being genuine BL Lacs. However, the percentage radio polarization may indicate some slight differences between these groups. In particular:

- The spectral indices at high radio frequencies indicate that the BL Lacs and candidate BL Lacs are indistinguishable, and that the sample of WLRG as a whole is statistically distinct from the BL Lacs in this regime.
- The candidate BL Lacs do however show a marginally steeper radio–optical spectra than the known BL Lacs. This is consistent with them being starlight–diluted BL Lacs in a sample limited in both optical and radio flux density.
- The candidate BL Lacs show a somewhat smaller polarization at radio wavelengths than the known BL Lacs. This could indicate they are slightly further from the line of sight, or that (possibly) they have a greater Faraday depth of depolarising medium.

The WLRG population of the 200 mJy sample is composed primarily of objects dominated by relativistically boosted cores and jets, which are probably closely related to the BL Lacs, as well as objects which just creep into the flat–spectrum sample with $\alpha_5^{1.4} < 0.5$, but whose spectra steepen more rapidly above 5 GHz. We confirm the result of MBIS that the BL Lacs have higher radio polarization cores compared to the WLRG, consistent with a simple interpretation as the WLRG being, on average, further from the line of sight. We also show that WLRG with highly polarized cores have flatter high frequency radio spectra, and suggest that these are the WLRG closest to the line of sight.

Within the WLRG population, we identify five objects which we believe to be strongly relativistically boosted. These objects are candidates for 'hidden BL Lacs': i.e. those objects physically identical to BL Lacs, at similar angles to the line of sight, but whose intrinsic power relative to their host galaxy makes them undetected as BL Lacs in the optical regime.

Acknowledgements. We thank Greg Taylor and Michael Rupen for help with the VLA scheduling. The National Radio Astronomy Observatory is a facility of the National Science Foundation operated under cooperative agreement by Associated Universities, Inc. This research was supported by the European Commission, TMR Programmme, Research Network Contract ERBFMRXCT96-0034 'CERES'.

References

Aller M.F., Aller H.D., Hughes P.A., Latimer G.E., 1999, ApJ 512, 601
Antonucci R., 1993, ARA&A 31, 473
Augusto P., Wilkinson P.N., Browne I.W.A., 1998, MNRAS 299, 1159
Barthel P.D., 1989, ApJ 336, 606
Blandford R.D., Konigl A., 1979, ApJ 232, 34
Bloom S.D., Marscher A.P., Gear W.K., et al., 1994, AJ 108, 398
Browne I.W.A., Marchã M.J.M., 1993, MNRAS 261, 795
Chiaberge M., Capetti A., Celotti A., 1999, A&A 349, 77
Condon J.J., Cotton W.D., Greisen E.W., et al., 1998, AJ 115, 1693
Cotton W.D., Feretti L., Giovannini G., Lara L., Venturi T., 1999, ApJ 519, 108
Dressler A., Shectman S.A., 1987, AJ 94, 899
Falcke H., Gopal-Krishna, Biermann P.L., 1995, A&A 298, 395
Fossati G., Celotti A., Ghisellini G., Maraschi L., 1997, MNRAS 289, 136
Gear W.K., Stevens J.A., Hughes D.H., et al., 1994, MNRAS 267, 167
Georganopoulos M., Marscher A.P., 1998, ApJ 506, 621
Ghisellini G., 1997, In: Relativistic Jets in AGNs. p. 262
Ghisellini G., Maraschi L., 1989, ApJ 340, 181
Ghisellini G., Padovani P., Celotti A., Maraschi L., 1993, ApJ 407, 65
Giovannini G., Taylor G.B., Arbizzani E., et al., 1999, ApJ 522, 101
Gregory P.C., Condon J.J., 1991, ApJS 75, 1011
Gregory P.C., Scott W.K., Douglas K., Condon J.J., 1996, ApJS 103, 427

Henstock D.R., Browne I.W.A., Wilkinson P.N., et al., 1995, ApJS 100, 1
Jackson C.A., Wall J.V., 1999, MNRAS 304, 160
Jackson N., Marchã M., 1999, MNRAS 309, 153
Kollgaard R.I., Wardle J.F.C., Roberts D.H., Gabuzda D.C., 1992, AJ 104, 1687
Lara L., Cotton W.D., Feretti L., et al., 1997, ApJ 474, 179
Laurent-Muehleisen S.A., Kollgaard R.I., Feigelson E.D., Brinkmann W., Siebert J., 1999, ApJ 525, 127
Maraschi L., Ghisellini G., Tanzi E.G., Treves A., 1986, ApJ 310, 325
Marchã M.J.M., Browne I.W.A., Impey C.D., Smith P.S., 1996, MNRAS 281, 425
Marscher A.P., 1980, ApJ 235, 386
Padovani P., Giommi P., 1995, ApJ 444, 567
Patnaik A.R., Browne I.W.A., Wilkinson P.N., Wrobel J.M., 1992, MNRAS 254, 655
Perlman E.S., Padovani P., Giommi P., et al., 1998, AJ 115, 1253
Pica A.J., Smith A.G., Webb J.R., et al., 1988, AJ 96, 1215
Puschell J.J., Stein W.A., 1980, ApJ 237, 331
Scheuer P., 1987, In: Zensus J., Pearson T. (eds.) Superluminal radio sources. Cambridge University Press, Cambridge, p. 104
Schoenmakers A.P., de Bruyn A.G., Röttgering H.J.A., van Der Laan H., 1999, A&A 341, 44
Snellen I.A.G., Zhang M., Schilizzi R.T., et al., 1995, A&A 300, 359
Stanghellini C., Dallacasa D., Bondi M., della Ceca R., 1997, A&A 325, 911
Stickel M., Fried J.W., Kuehr H., Padovani P., Urry C.M., 1991, ApJ 374, 431
Stickel M., Kuehr H., Fried J.W., 1993, A&AS 97, 483
Stocke J.T., Liebert J., Schmidt G., et al., 1985, ApJ 298, 619
Stocke J.T., Morris S.L., Gioia I.M., et al., 1991, ApJS 76, 813
Tapia S., Craine E.R., Johnson K., 1976, ApJ 203, 291
Taylor G.B., Vermeulen R.C., Pearson T.J., et al., 1994, ApJS 95, 345
Urry C.M., Padovani P., 1995, PASP 107, 803
Venturi T., Giovannini G., Feretti L., Comoretto G., Wehrle A.E., 1993, ApJ 408, 81
White R.L., Becker R.H., 1992, ApJS 79, 331
White R.L., Becker R.H., Helfand D.J., Gregg M.D., 1997, ApJ 475, 479
Wilkinson P.N., Browne I.W.A., Patnaik A.R., Wrobel J.M., Sorathia B., 1998, MNRAS 300, 790